

# Guided Exploration of Human Intentions for Human-Robot Interaction

Min Chen, David Hsu, and Wee Sun Lee

National University of Singapore, Singapore 117417, Singapore

**Abstract.** Robot understanding of human intentions is essential for fluid human-robot interaction. Intentions, however, cannot be directly observed and must be inferred from behaviors. We learn a model of adaptive human behavior conditioned on the intention as a latent variable. We then embed the human behavior model into a principled probabilistic decision model, which enables the robot to (i) explore actively in order to infer human intentions and (ii) choose actions that maximize its performance. Furthermore, the robot learns from the demonstrated actions of human experts to further improve exploration. Preliminary experiments in simulation indicate that our approach, when applied to autonomous driving, improves the efficiency and safety of driving in common interactive driving scenarios.

## 1 Introduction

Understanding human intentions is essential for fluid human-robot interaction. It helps the robot to interpret humans' behaviors and predict their future actions. Earlier work often treats humans as passive moving obstacles in the environment: humans do not react to robot actions [3,4,10]. As a result, the robot is overly conservative. It waits and observes until humans' intentions become clear. However, in reality, humans are not merely moving obstacles, and they respond to robot actions. For example, in our study of lane-switch for autonomous driving, a robot car tries to switch to a lane, in which a human-driven car drives (Fig. 1). A conservative human driver will slow down, while an aggressive driver will accelerate and refuse to let the robot car in. If the robot car chooses to wait, the human driver will maintain the speed, and the robot car will not learn the human driver's intention. Human intentions, human actions, and robot actions are interconnected. The robot must take advantage of the connections and actively *explore* in order to understand human intentions.

Exploration is, however, not always appropriate. Consider the lane-switch example again (Fig. 1d). If the robot car switches lanes when the two cars are very close, the human will not have enough time to react. In our study, the participants indicated that they felt unsafe in such situations. So the robot must not only explore, but also explore safely, for effective human-robot interaction.

To this end, we propose two ideas. The first is an intention-driven human behavior model, integrated into a probabilistic robot decision making framework

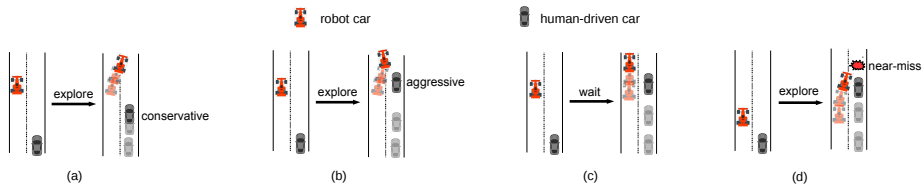


Fig. 1: A robot car explores human intentions during the lane-switch. (a,b) If the robot car tries to explore, a conservative human driver will slow down, while an aggressive human driver may accelerate, revealing the human intentions. (c) If the robot car chooses to wait, the human driver will maintain the speed. The robot car will not learn the human driver’s intention and initiate the lane switch suitably. (d) Exploration may be dangerous, when the two car are too close.

for human-robot interaction. Unlike earlier work on intentional behavior modeling [3], our model conditions human actions explicitly on robot actions and captures *adaptive* human behaviors. Since the human intention is not directly observable, we model it as a latent variable in a partially observable Markov decision process (POMDP) [13]. We further assume that the human intention remains static during a single interaction, thus reducing the POMDP model to a computationally more efficient variant, POMDP-lite [6]. Despite the simplifying assumption, the resulting intention POMDP-lite model successfully captures many interesting human behaviors. See Section 5 for examples. Handcrafting accurate POMDP models is a major challenge. Here we take a data-driven approach and learn the intention POMDP-lite model from data. Solving an intention POMDP-lite model produces a policy that enables the robot to explore actively and infer human intentions in order to improve robot performance.

Aggressive exploration is sometimes unsafe in applications such as driving. Our second idea is to leverage human expert demonstrations for improved robot exploration. We learn from human demonstrations a probability distribution over state-action pairs. The learned distribution captures the actions of human experts when exploration is needed. It is then used as a heuristic to guide robot exploration and favor the frequently demonstrated state-action pairs.

We evaluated our approach in simulation on common driving tasks, including lane-switch and intersection navigation. Compared with a myopic policy that does not actively explore human intentions, intention POMDP-lite substantially improved robot driving efficiency. Combined with guided exploration, it also improved driving safety. While our experiments are specific to autonomous driving, the approach is general and applicable to other human-robot interaction tasks that require exploration of human intentions.

In the following, Section 2 briefly surveys related work. Section 3 presents the intention POMDP-lite model and guided exploration. Section 4 describes how we learn an intention-driven human driving policy and a distribution for guided exploration. Section 5 compares our approach with common alternatives in simulation. Section 6 discusses the limitations of the current approach and directions for further investigation.

## 2 Related Work

Intention has been studied extensively in the field of psychology [2,5], where intention is characterized as a mental state that represents human’s commitment to carrying out a sequence of actions in the future. Understanding intentions is crucial in understanding various social contexts, e.g., it helps to interpret other people’s behaviors and predict their future actions [9].

In human-robot interaction, intention has been used as a means to model human behaviors [18,3,4,24,16]. For example, Bai et al. [3] modeled pedestrians’ behaviors with a set of intentions, and they enabled the autonomous car to drive successfully in a crowd. However, they assumed that the human won’t react to the robot, which made the robot act conservatively most of the time. Most recently, Sadigh et al. [22] showed that robot’s action directly affects human actions, which can be used to actively infer human intentions [23]. However, inferring human intentions is not the end goal. Instead, our work embeds an intention-driven human behavior model into a principled robot decision model to maximize the robot performance. In other words, the robot may choose to ignore the human if he/she does not affect robot performance.

To maximize performance, the robot needs to actively infer human intentions (exploration), and achieve its own goal (exploitation). In addition, the robot needs to explore gently as the human might not willing to be probed in certain scenarios. The partially observable Markov decision process (POMDP) [13] trades off exploration and exploitation optimally. However, POMDP itself does not model human’s intent to be probed, thus it may generate explorative actions that are too aggressive. Imitation learning derives a robot policy directly from human demonstrations [1]. But the robot policy cannot be generalized to unseen state space. Instead of learning a robot policy directly, Garcia et al. [11] used human demonstrations to guide robot explorations, and they significantly reduced the damage incurred from exploring unknown state-action space. Our work draws insight from [11], and we explicitly guide robot explorations in a POMDP model with human demonstrations.

## 3 Intention POMDP-lite with Guided Exploration

### 3.1 Mathematical Formulation of Human-Robot Interaction

Mathematically, we formulate the human-robot interaction problem as a Markov decision process  $(X, A^R, A^H, T, R^R, R^H, \gamma)$ , where  $x \in X$  is the world state.  $A^R$  is the set of actions that the robot can take, and  $A^H$  is the set of actions that the human can take. The system evolves according to a stochastic state transition function  $T(x, a^R, a^H, x') = P(x'|x, a^R, a^H)$ , which captures the probability of transitioning to state  $x'$  when joint actions  $(a^R, a^H)$  are applied at state  $x$ . At each time step, the robot receives a reward of  $r^R(x, a^R, a^H)$  and the human receives a reward of  $r^H(x, a^R, a^H)$ . The discount factor  $\gamma$  is a constant scalar that favors immediate rewards over future ones.

Given a human behavior policy, i.e.,  $a^H \sim \pi^H$ , the optimal value function of the robot is given by Bellman’s equation

$$V^*(x|\pi^H) = \max_{a^R} \left\{ \mathbb{E}_{a^H \sim \pi^H} \left[ r^R(x, a^R, a^H) + \sum_{x'} \gamma P(x'|x, a^R, a^H) V^*(x'|\pi^H) \right] \right\} \quad (1)$$

The optimal robot policy  $\pi_*^R$  is the action that maximizes the right hand side of Equation 1, and the key to solve it is to have a model of human behaviors.

### 3.2 Intention-Driven Human Behavior Modeling

Our insight in modeling human behaviors is that people cannot be treated as obstacles that move, i.e., people select actions based on their *intentions* and they *adapt* to what the robot does.

Following previous works on intention modeling [4,22], we assume that human intention can be represented as a single discrete random variable  $\theta$ , and we explicitly condition human actions on their intention, i.e.,  $a_t^H \sim \pi^H(a_t^H|x_t, \theta_t)$ .

Apart from their own intention, people also adapt to the robot. In the most general case, people condition their actions on the entire human-robot interaction history, i.e.,  $h_t = \{a_0^R, a_0^H, \dots, a_{t-1}^R, a_{t-1}^H\}$ . However, the history  $h_t$  may grow arbitrary long and make human actions extremely difficult to compute. Even if we can compute it, this will still not be a good model for how people make decisions in day to day tasks since people are known to be not fully rational, i.e., bounded rationality [21,14]. In human-robot interaction, bounded rationality has been modeled by assuming that people have “bounded memory”, and they based their decisions only on most recent observations [17].

Our human behavior model connects the human intention model with the bounded memory model, i.e., people condition their actions on their intention and the last  $k$  steps of the history,  $h_t^k = \{a_{t-k}^R, a_{t-k}^H, \dots, a_{t-1}^R, a_{t-1}^H\}$ . Thus, the human behavior policy can be rewritten as

$$a_t^H \sim \pi^H(a_t^H|x_t, h_t^k, \theta_t) \quad (2)$$

### 3.3 Intention POMDP-lite

A key challenge is that human intention can not be directly observed by the robot, and therefore has to be inferred from human behaviors. To achieve that, We model human intention as a latent state variable in a partially observable Markov decision process (POMDP). In this paper, we assume the human intention remains static during a single interaction. Thus, we can reduce the POMDP model to a POMDP-lite model [6], which can be solved more efficiently.

To build the intention POMDP-lite model, we first create a factored state  $s = (x, \theta)$  that contains the fully observable world state  $x$  and the partially observable human intention  $\theta$ . We maintain a belief  $b$  over human intention. The human behavior policy is embedded in the POMDP-lite transition dynamics, and we describe in Section 4 how we learn it from data. Fig. 2 shows the intention POMDP-lite graphical model and human-robot interaction flowchart.

The solution to an intention POMDP-lite is a policy that maps belief states to robot actions, i.e.,  $a_t^R = \pi^R(b_t, x_t)$ . And it has two distinct objectives: (1)

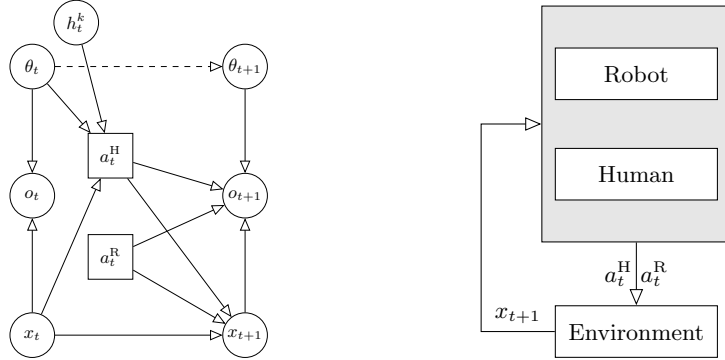


Fig. 2: The intention POMDP-lite graphical model and the human-robot interaction flowchart. The robot action  $a_t^R$  depends on the world state  $x_t$  and the belief over human intention  $\theta_t$ . The dashed arrow indicates the static assumption on the intention dynamics, i.e.,  $\theta_t = \theta_{t+1}$ .

maximizing rewards based on current information (exploitation); (2) gathering information over human intention (exploration).

The Bayes-optimal robot trades off exploration/exploitation by incorporating belief updates into its plans [8]. It acts to maximize the following value function

$$V^*(b_t, x_t) = \max_{a_t^R} \left\{ r^R(b_t, x_t, a_t^R) + \sum_{x_{t+1}} \gamma P(x_{t+1}|b_t, x_t, a_t^R) V^*(b_{t+1}, x_{t+1}) \right\} \quad (3)$$

where  $r^R(b_t, x_t, a_t^R) = \sum_{\theta_t} b_t(\theta_t) P(a_t^H|\theta_t) r^R(x_t, a_t^R, a_t^H)$  is the mean reward function, and  $P(x_{t+1}|b_t, x_t, a_t^R) = \sum_{\theta_t} b_t(\theta_t) P(a_t^H|\theta_t) P(x_{t+1}|x_t, a_t^R, a_t^H)$  is the mean transition function, where  $P(a_t^H|\theta_t)$  depends on the human behavior policy in Equation 2. Note that  $b_{t+1} = \tau(b_t, a_t^R, x_{t+1})$  is the updated belief after arriving at a new state  $x_{t+1}$ , where  $\tau$  represents Bayes' rule.

However, Bayes-optimal planning is intractable in general. An alternative approach to trade off exploration/exploitation is the explicit modification of the reward function, i.e., adding an extra reward bonus for exploration [6]. In this case, the robot acts to maximize the following value function:

$$\tilde{V}^*(b_t, x_t) = \max_{a_t^R} \left\{ \beta r^B(b_t, x_t, a_t^R) + r^R(b_t, x_t, a_t^R) + \sum_{x_{t+1}} \gamma P(x_{t+1}|b_t, x_t, a_t^R) \tilde{V}^*(b_t, x_{t+1}) \right\} \quad (4)$$

where  $r^B(b_t, x_t, a_t^R)$  is the reward bonus term that encourages the robot to explore.  $\beta$  is a constant scalar that explicitly trades off exploration and exploitation. Note that the belief  $b_t$  is not updated in this equation. In other words, solving Equation 4 is equivalent to solving a mean MDP of current belief with an additional reward bonus, which is computationally efficient. More impor-

tantly, the computed robot policy is near Bayes-optimal [6], given that the reward bonus is defined as the expected  $L_1$  distance between two consecutive beliefs  $\mathbb{E}_{b_{t+1}} \|b_{t+1} - b_t\|_1$ .

### 3.4 Guided Exploration

The policy computed by Equation 4 enables the robot to actively infer human intentions, however, the human might not like to be probed in certain scenarios (e.g., Fig. 1d). Thus, guidance needs to be provided for more effective robot explorations.

We achieve guided exploration via human expert demonstrations. More specifically, we maintain a probability distribution over each state-action pair, where  $p^G(x, a^R) \in [0, 1]$  measures how likely the human expert will take action  $a^R$  at state  $x$ . We will describe in Section 4 how we learn  $p^G(x, a^R)$  from data. The learned probability distribution is then embedded into the reward bonus term as a prior knowledge, and our algorithm acts to maximize the following value function:

$$\tilde{V}^{G^*}(b_t, x_t) = \max_{a_t^R} \left\{ \beta p^G(x_t, a_t^R) r^B(b_t, x_t, a_t^R) + r^R(b_t, x_t, a_t^R) + \sum_{x_{t+1}} \gamma P(x_{t+1} | b_t, x_t, a_t^R) \tilde{V}^{G^*}(b_t, x_{t+1}) \right\} \quad (5)$$

Compared with Equation 4, the reward bonus term is multiplied by  $p^G(x_t, a_t^R)$ , which discourages robot exploration when  $p^G(x_t, a_t^R)$  is small. Although we discourage the robot to explore certain state action pairs, the theoretic results in the POMDP-lite paper [6] retains, i.e., the robot policy remains near Bayes-optimal. The proof of the theorem is deferred to the appendix.

**Theorem 1.** *Let  $\mathcal{A}_t$  denote the policy followed by our algorithm at time step  $t$ . Let  $x_t, b_t$  denote the state and belief at time step  $t$ . Let  $|X|, |A^R|$  denote the size of the state space and robot action space. Let  $\phi$  denote the minimal value of the probability distribution  $p^G(x, a^R)$ , i.e.,  $\phi = \min\{p^G(x, a^R)\}$ . Suppose  $\phi > 0$ ,  $\beta = O(\frac{|X|^2, |A^R|}{\phi(1-\gamma)^2})$ , for any inputs  $\forall \delta > 0, \epsilon > 0$ , with probability at least  $1 - \delta$ ,*

$$V^{\mathcal{A}_t}(b_t, x_t) \geq V^*(b_t, x_t) - 4\epsilon.$$

In other words, our algorithm is  $4\epsilon$ -close to the Bayes-optimal policy, for all but  $m = O(\text{poly}(|X|, |A^R|, \frac{1}{\epsilon}, \frac{1}{\delta}, \frac{1}{1-\gamma}))$  time steps.

## 4 Learning Human Behavior Policies and Guided Robot Exploration

Nested within the intention POMDP-lite model is the human behavior policy  $\pi^H(a_t^H | x_t, h_t^k, \theta_t)$ , and the guided exploration distribution  $p^G(x_t, a_t^R)$ . We adopt a data-driven approach and learn those two models from data for the interactive



Fig. 3: Simulation setup. (a) A human driver interacts with a robot car in the driving simulator powered by the Unity 3D engine. (b,c,d) Three interactive driving tasks: lane-switch, intersection, and lane-merge.

driving tasks. Note that suitable probabilistic models derived from alternative approaches can be substituted for these learned models.

#### 4.1 Data Collection

**Interactive driving tasks.** Fig. 3 shows the simulation setup and three typical interactive driving tasks. For simplicity, we assume both the human-driven car and the robot car follow a fixed path respectively. For example, in the intersection scenario, each of them will follow a path that goes straight forward. With this assumption, the human driver and the robot only need to control the speed of the vehicles. The steering angle is controlled by a path tracking algorithm [7]. One exception is the lane-switch scenario, where the robot can decide when to switch lanes, and has two additional actions, i.e.,  $\{switch-left, switch-right\}$ . Once the robot decides to switch lanes, a new path will be generated online and the path tracking algorithm will start following the new path.

In general, human intention in driving scenarios has multiple dimensions, e.g., turn-left/turn-right, aggressive/conservative, e.t.c. In this paper, we focus on the last dimension, i.e., the human driver can be either aggressive or conservative.

**Participants.** We recruited 10 participants (3 female, 7 male) in the age range of 22 – 30 years old. All participants owned a valid driving license.

**Design.** The human-driven car was controlled by one of the participants, and the robot car was controlled by a human expert. Note that the human expert was not recruited from the general public but one of the experiment conductors. Intuitively, one can treat the participants as the human drivers that the robot will interact with, and the human expert as the owner of robot car whom teaches the robot how to act in different scenarios.

We learn a human drivers’ behavior model from the controls recorded from the participants. To capture different human intentions, we asked each participant to perform the task as an aggressive human driver and as a conservative human driver. Note that the notion of “aggressive/conservative” is subjective and may vary among different participants. Thus, we expect certain amount of variance in our human behavior prediction model.

Similarly, we learn a guided exploration distribution from the controls recorded from the human expert. Since safety is our primary concern in the driving tasks, the human expert was told to drive carefully.

**Procedure.** Before the simulation started, the participant was asked to follow one of the driver intentions, i.e., aggressive or conservative. Once the simulation started, the participant and the human expert could control the speed of their vehicles respectively via an accelerator pedal that provides continuous input. In the lane-switch scenario, the human expert could also decide when to switch to the other lane. The simulation ends once the robot car has achieved its goal, i.e., crossed the intersection or switched to another lane.

**Data format.** The world state in the driving task is depicted in Fig. 4,  $x = \{d^H, d^R, v^H, v^R\}$ , where  $d^H, d^R$  are the vehicles’ distance to the potential colliding point, and  $v^H, v^R$  are the vehicles’ current speed.

For each simulation sequence, we recorded two set of data,  $\mathbb{D}_i^H$  and  $\mathbb{D}_i^G$ , for learning the human behavior model and guided exploration distribution respectively. The data recorded can be written as follows:

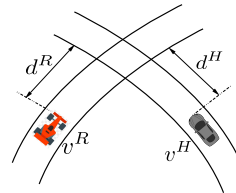


Fig. 4: The world state for an interactive driving task.

$$\mathbb{D}_i^H = \theta_i \cup \{(x_0, a_0^R, a_0^H), \dots, (x_{K_i}, a_{K_i}^R, a_{K_i}^H)\}, \quad \mathbb{D}_i^G = \{(x_0, a_0^R), \dots, (x_{K_i}, a_{K_i}^R)\}$$

where  $\theta_i$  is the human intention at the  $i$ th interaction,  $K_i$  is the number of steps in the  $i$ th interaction.  $x_t$  is the world state at time step  $t$ .  $v_t^R, a_t^R$  are the speed and acceleration of the robot car at time step  $t$ .  $v_t^H, a_t^H$  are the speed and acceleration of the human-driven car at time step  $t$ .

Each participant was asked to perform the driving task 8 times as an aggressive driver and 8 times as a conservative driver. We have 10 participants in total, this gives us 160 sequences of interactions for the learning purpose, i.e., 80 for the aggressive human driver, 80 for the conservative human driver, and 160 for the guided exploration distribution.

## 4.2 Human Behavior Policy

A human behavior policy is a function that maps the current world state  $x_t$ , bounded history  $h_t^k$  and human intention  $\theta_t$  to human actions (Equation 2), where human actions are accelerations in our driving tasks. The Gaussian Process (GP) places a distribution over functions. It serves a non-parametric form of interpolation, and it is extremely robust to unaligned noisy measurements [20]. In this paper, we use GP as the human behavior prediction model.

We learn a GP model for each human driver type, i.e., aggressive or conservative. Our GP model is specified by a set of mean and covariance functions, whose input includes the world state  $x_t$  and bounded history  $h_t^k$ , i.e.,  $\mathbf{x} = (x_t, h_t^k)$ . To fix the dimension of the input, we add paddings with value of 0 to the history if  $t < k$ .

**Mean function.** The mean function is a convenient way of incorporating prior knowledge. We denote the mean function as  $\mu(\mathbf{x})$ , and set it initially to be the mean of the training data. This encodes the prior knowledge that, without any



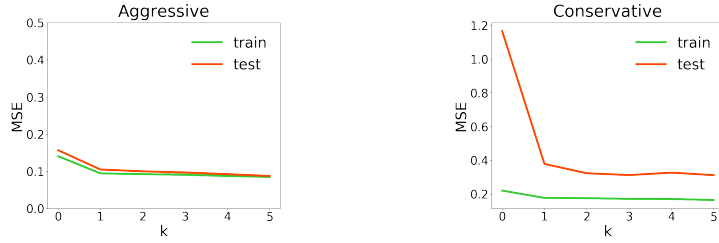


Fig. 5: The Mean Squared Error (MSE) of GP predictions with increasing history length  $k$ . The MSE stabilizes for  $k \geq 2$ , confirming that humans have short, bounded memory in driving tasks.

additional knowledge, we expect the human driver to behave similarly to the average of what we have observed before.

**Covariance function.** The covariance function describes the correlations between two inputs,  $\mathbf{x}$  and  $\mathbf{x}'$ , and we use the standard radial-basis function kernel [25].

$$k(\mathbf{x}, \mathbf{x}') = \exp \left( -1/2 \left( \left( \frac{d^H - d^{H'}}{\sigma_d} \right)^2 + \left( \frac{d^R - d^{R'}}{\sigma_d} \right)^2 + \left( \frac{v^H - v^{H'}}{\sigma_v} \right)^2 + \left( \frac{v^R - v^{R'}}{\sigma_v} \right)^2 + \sum_{a^R, a^H \in h_t^k} \left( \left( \frac{a^R - a^{R'}}{\sigma_a} \right)^2 + \left( \frac{a^H - a^{H'}}{\sigma_a} \right)^2 \right) \right) \quad (6)$$

where the exponential term encodes that similar state and history should make similar predictions. The length-scale  $\sigma_d$ ,  $\sigma_v$  and  $\sigma_a$  normalize the scale of the data, i.e., distance, speed and acceleration.

**Training.** We train the GP model with the scikit-learn package [19], where 80% data is used for training and 20% data is used for testing. We evaluate different values of  $k$ . Fig. 5 shows the mean squared train/test error with respect to  $k$ . The errors are large when  $k = 0$  (people ignore the robot), but converge quickly within 2 steps. This supports our intuition that people adapt to the robot but have a bounded memory. In the remainder of the paper, GP models with  $k = 2$  are used to predict human actions.

Fig. 6 shows GP predictions for some example scenarios. The plots are generated by varying one of the input variables, i.e.,  $d$  or  $v$ , while fixing the others. Due to space constraints, we only show selected plots where the aggressive human driver and the conservative human driver are most distinguishable. The key message in those plots is: the conservative human driver slows down if there is a potential collision in the near future, while the aggressive human driver keeps going and ignores the danger. The robot can take advantage of this difference to actively infer human intentions.

**Human behavior policy table.** The human behavior policy will be queried frequently during the robot planning phase, and GP prediction is too slow for online POMDP planning. Instead, we build a policy table offline for each human

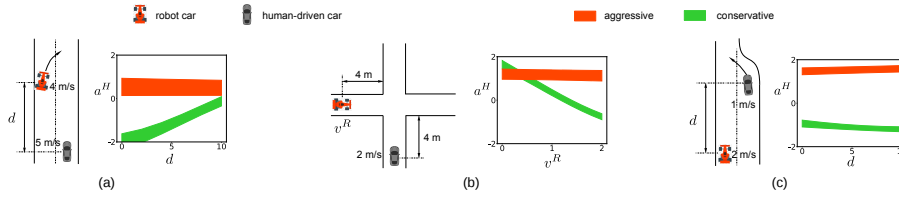


Fig. 6: GP predictions of human accelerations, mean and standard error ( $y$  axis), for some example driving scenarios. (a) Predicted human acceleration w.r.t the distance between two vehicles (lane-switch). (b) Predicted human acceleration w.r.t the velocity of the robot car (intersection). (c) Predict human acceleration w.r.t the distance between two vehicles (lane-merge).

driver type, where we store all the GP predictions. During the online phase, the POMDP planning algorithm only needs to query the table and it is much faster.

To build a policy table, we discretize the state space and action space as follows:

- Distance (m): near  $[0, 5)$ , middle  $[5, 20)$ , far  $[20, +\infty)$ .
- Speed (m/s): low  $[0, 1)$ , middle  $[1, 5)$ , high  $[5, +\infty)$ .
- Acceleration ( $\text{m/s}^2$ ): decelerate  $(-\infty, -0.2)$ , keep  $[-0.2, 0.2]$ , accelerate  $(0.2, +\infty)$ .

With this level of discretization, the policy table will have  $3^8$  entries when history length  $k = 2$ .

### 4.3 Probability Distribution for Guided Exploration

For the autonomous driving task, we are mostly concerned with a state-action pair being safe or unsafe. Consequently, the probability  $p^G(x, a^R)$  measures how safe it is for the robot to explore  $(x, a^R)$ , i.e., safe probability.

**Prior.** Since a state-action pair is either safe or unsafe, a natural means is to use Beta distribution as a prior, i.e.,  $Beta(\alpha(x, a^R), \beta(x, a^R))$ . The initial safe probability can be computed as

$$p^G(x, a^R) = \frac{\alpha(x, a^R)}{\alpha(x, a^R) + \beta(x, a^R)}$$

Initially, we set  $\alpha(x, a^R) = 0.05, \beta(x, a^R) = 5, \forall x \in X, a^R \in A^R$ . This implies that all state-action pairs are close to unsafe without seeing any human demonstrations.

**Posterior.** Given a set of human demonstration data  $\mathbb{D}^G = \{(x_0, a_0^R), \dots, (x_N, a_N^R)\}$ , the posterior of the safe probability can be computed as

$$\tilde{p}^G(x, a^R) = \frac{\alpha(x, a^R) + n(x, a^R)}{\alpha(x, a^R) + \beta(x, a^R) + n(x, a^R)}$$

where  $n(x, a^R)$  is the number of times that  $(x, a^R)$  appeared in the human demonstration data.

**Safe probability table.** Similar to the human behavior policy, we store all the safe probabilities in a table, and we follow the same discretization intervals for the human behavior policy table.

## 5 Simulation Experiments

Our approach, intention POMDP-lite with Guided exploration (IPL-G), enables the robot to actively infer human intentions and choose explorative actions that are similar to the human expert. In this section, we present some simulation results on several interactive driving tasks, where the robot car interacts with a simulated human driver. We sought to answer the following two questions:

- **Question A.** Does active exploration improve robot efficiency?
- **Question B.** Does guided exploration improve robot safety?

**Comparison.** To answer question A, we compared IPL-G with a myopic robot policy that does not actively explore, i.e., the reward bonus in Equation 4 was set to be 0. To answer question B, we compared IPL-G with the original intention POMDP-lite model (IPL) without guided exploration.

Since the driving scenarios considered in this paper are relatively simple, one may argue that a simple heuristic policy might work just as well. To show that is not the case, we designed an additional baseline, i.e., heuristic- $k$ , and it works as follows: the robot explores at the first  $k$  steps, e.g., accelerate or switch lane, then the robot proceeds to go if the human slows down, otherwise, the robot waits until the human has crossed.

**Parameter settings.** Both IPL and IPL-G need to set a constant scalar  $\beta$  that trades off exploration and exploitation (Equation 4 and Equation 7). Similar to previous works [15], we evaluated a wide range of values for  $\beta$ , and chose the one that had the best performance on IPL. In this way,  $\beta$  favors IPL more than IPL-G.

For the heuristic policy, we need to choose parameter  $k$ , i.e., the number of steps that robot explores at the beginning. We evaluated heuristic policies with different values of  $k \in \{1, 2, 3, 4\}$ , and chose the one that had the best performance.

**Performance measures.** To measure the efficiency of a policy, we used the time taken for the robot to achieve its goal as the performance measure, i.e.,  $T(goal)$ , the less the better.

To measure the safety of a policy, we used the near-miss rate as the performance measure, i.e.,  $P(near - miss)$ , since we didn't observe any accidents in the simulations. We adopted the definition of near-miss from a seminal paper in the field of traffic safety control [12], where near-miss was defined based on the time-measured-to-collision (TMTC). TMTC is the time required for the two vehicles to collide if they continue at their current velocity. Intuitively, TMTC is a measurement of danger, and lower TMTC value implies that the scenario is more dangerous. According to [12], a near-miss happens if the value of TMTC is

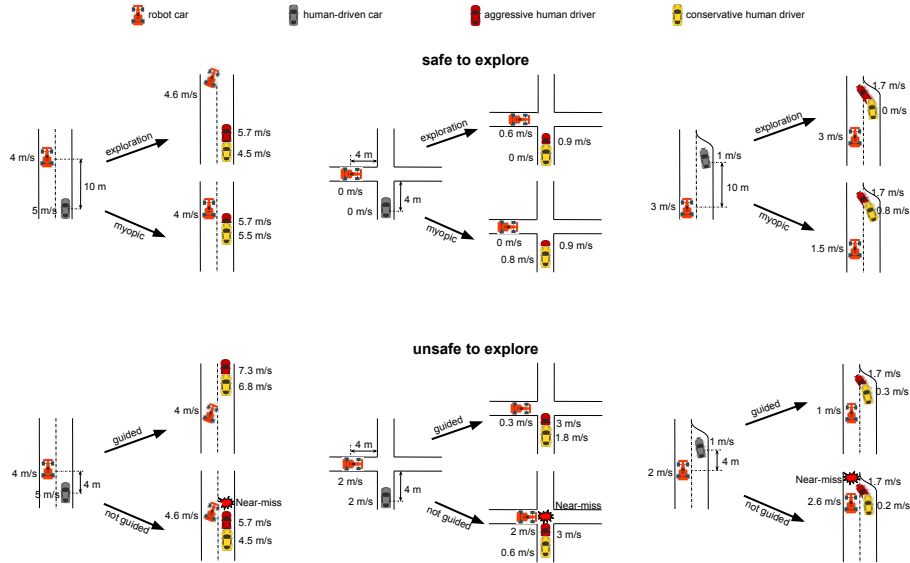


Fig. 7: Top row: comparison of the active exploration policy and the myopic policy, when exploration is safe. Bottom row: comparison of policies with and without guided exploration, when exploration is unsafe.

lower than 1 second, and an analysis over the films taken with the surveillance system at an urban interaction suggested a near-miss rate of **0.35** in daily traffic.

**Simulation setup.** For all the simulations performed, the robot car was controlled by one of the algorithms above. The human-driven car was controlled by learned human behavior policy in Section 4.2. For each simulation run, the human driver was set to be aggressive or conservative with 0.5 probability.

The state space  $x$  was set to be continuous. The robot action space was set to be discrete, i.e., {Accelerate, Keep, Decelerate}, which controls the speed of the car. The steering angle of the car was controlled independently by a path tracking algorithm [7]. All planning algorithms were given 0.33 second per step to compute the robot actions online.

### 5.1 Driving Scenarios

To test the effectiveness of active exploration, we selected three interactive driving scenarios where robot exploration is safe (Fig. 7, top row). Initially, the robot car either had a safe distance to the human-driven car or had low speed. This gave the robot car enough space/time to explore without too much danger of colliding to the human-driven car. The myopic robot waited until the human-driven car had crossed or slowed down. However, the active exploration robot started to switch to the other lane or accelerate to test if the human was willing to yield. If the human was conservative and slowed down, the robot proceeded to go and improved its efficiency.

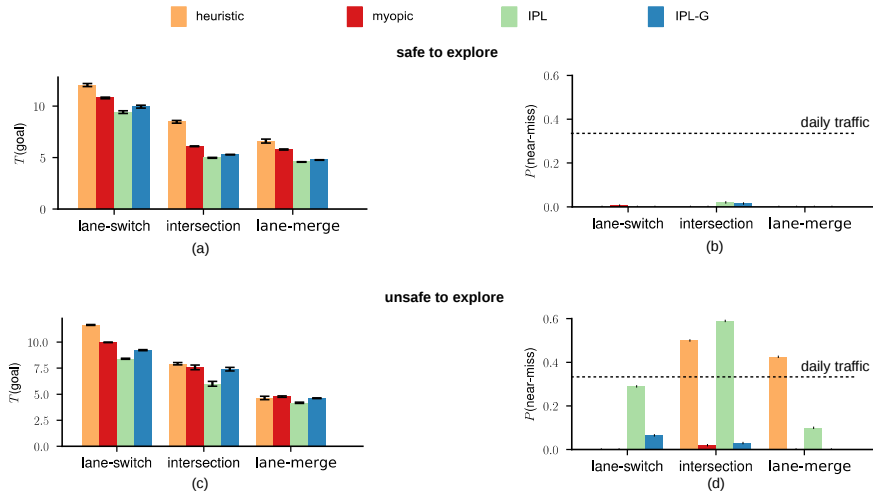


Fig. 8: Performance results. Top row: when it was safe to explore, the active exploration policy (IPL and IPL-G) achieved better efficiency with nearly zero near-misses. Bottom row: when it was unsafe to explore, the IPL-G robot achieved significantly lower near-miss rate compared with the robot that explores without guided exploration (IPL).

To test the effectiveness of guided exploration, we selected another three interactive driving scenarios where robot exploration is unsafe (Fig. 7, bottom row). Initially, the robot car was near to the human-driven car and it had high speed. Without guided exploration, the IPL robot chose to switch lane or cross the intersection, which might cause near-misses. On the other hand, with guided exploration, the IPL-G robot chose to not explore and waited for the human to cross first.

## 5.2 Quantitative Results

We performed 200 simulation runs for each scenario. The performance results are shown in Fig. 8.

When robot exploration was safe, both IPL and IPL-G actively explored. This significantly reduced the time taken for the robot to achieve its goal, compared with the robot that followed a myopic policy or a heuristic policy (Fig. 8a). Very few near-misses ( $< 0.02$ ) have been observed for all the robot policies, which supports our intuition that it is safe for the robot to explore in those scenarios (Fig. 8b). Note that the dashed line represents the near-miss rate in daily traffic, which is adopted from a seminal paper in traffic safety control [12]. It helps us to calibrate the safety levels of different algorithms.

When robot exploration was unsafe, The IPL robot was aggressive at gathering information. This indeed made the robot car more efficient (Fig. 8c). However, this is counterbalanced by the fact that it also led to a lot of near-misses (Fig. 8d). The IPL robot incurred more near-misses than the daily traffic in

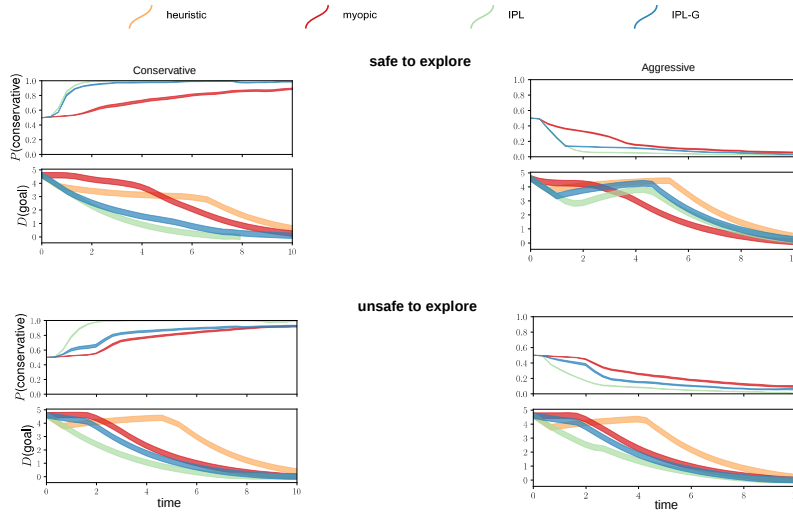


Fig. 9: Averaged robot trajectories in the lane-switch scenario. The plots show the mean and standard error of the belief  $P(\text{conservative})$  and the remaining distance to the robot goal  $D(\text{goal})$ , with respect to time.

the intersection scenario, and it had significantly higher near-miss rate than the IPL-G robot across all tasks, which supports our intuition that guided exploration can significantly improve robot safety in driving tasks. The heuristic policy explored at the first 2 steps, which already caused a lot of near-misses. This implies that arbitrary exploration is dangerous in general, and should not be encouraged.

We use the averaged robot trajectories from the lane-switch task as an example to illustrate the robot policies from different algorithms. (Fig. 9). When it was safe to explore (Fig. 9, top row), the IPL robot and the IPL-G robot were able to identify human intentions quickly, i.e., the belief  $P(\text{conservative})$  converged to 1 or 0 quickly. Consequently, if the human was conservative, the robot proceeded to go and improved its efficiency, i.e.,  $D(\text{goal})$  decreased faster than the myopic robot. When it was unsafe to explore (Fig. 9, bottom row), guided exploration prevented the IPL-G robot to explore, i.e., its belief  $P(\text{conservative})$  converged slower than the belief of the IPL robot (without guided exploration). Consequently, the IPL-G robot was less aggressive and it encountered significantly less near-misses compared to the IPL robot (Fig. 8d).

## 6 Discussion

Intention POMDP-lite embeds a learned human behavior model in a probabilistic decision framework. It is task-driven and gathers information on human intentions only when necessary to improve task performance. The simulation experiments suggest that active exploration enables the robot car to infer human

intentions more effectively and improve driving performance, compared with the myopic policy. By leveraging expert demonstration data, guided exploration biases exploration in promising directions and prevents exploration when it is ineffective or unsafe. Overall, intention POMDP-lite with guided exploration tries to answer the question of *how* and *when* to perform active exploration in human-robot interactive tasks. The diverse robot behaviors emerge automatically from the decision framework, without the kind of explicit manual programming required for heuristic driving policies.

Although our experiments are specific to autonomous driving, understanding human intentions is essential in a wide range of human-robot interaction tasks, and our overall approach is generally applicable. For example, a kitchen assistant robot tries to understand the recipe that a human tries to follow and helps by preparing the ingredients. Similarly, a robot tries to understand a human’s plan for assembling a piece of furniture and gathers the parts and tools required. In these settings, the risk of exploration may not be safety, but potentially negative impact on task performance.

The current work has several limitations that require further investigation. One important issue is human intention modeling. We treat intention as a single discrete random variable. Specifically, our current experiment design considers only two intentions: aggressive or conservative. The simplified intention model allows us to analyze the core technical issues without the interference of confounding factors. In reality, human drivers may exhibit a mixture of aggressive and conservative behaviors. A multi-dimensional, continuous parameterization would provide a richer and more accurate intention representation. In addition, we assume that intention is static, while it may change over time. We expect our approach to be robust against intention changes, as online planning handles unexpected changes naturally, but we plan to conduct a human subject study to examine this issue further.

**Acknowledgments.** This work is supported in part by the Singapore NRF through the SMART Future Urban Mobility IRG and MOE AcRF grant MOE2016-T2-2-068.

## References

1. Abbeel, P., Ng, A.Y.: Apprenticeship learning via inverse reinforcement learning. In: Proc. Int. Conf. on Machine Learning. p. 1. ACM (2004)
2. Astington, J.W.: The child’s discovery of the mind, vol. 31. Harvard University Press (1993)
3. Bai, H., Cai, S., Ye, N., Hsu, D., Lee, W.S.: Intention-aware online pomdp planning for autonomous driving in a crowd. In: Proc. IEEE Int. Conf. on Robotics & Automation. pp. 454–460. IEEE (2015)
4. Bandyopadhyay, T., Won, K.S., Frazzoli, E., Hsu, D., Lee, W.S., Rus, D.: Intention-aware motion planning. In: Proc. Int. Workshop on the Algorithmic Foundations of Robotics, pp. 475–491. Springer (2013)
5. Bratman, M.: Intention, plans, and practical reason. Harvard University Press, Cambridge, MA (1987)

6. Chen, M., Frazzoli, E., Hsu, D., Lee, W.S.: Pomdp-lite for robust robot planning under uncertainty. In: Proc. IEEE Int. Conf. on Robotics & Automation. pp. 5427–5433. IEEE (2016)
7. Coulter, R.C.: Implementation of the pure pursuit path tracking algorithm. Tech. rep., Carnegie-Mellon UNIV Pittsburgh PA Robotics INST (1992)
8. Duff, M.O.: Design for an optimal probe. In: Proc. Int. Conf. on Machine Learning. pp. 131–138 (2003)
9. Feinfield, K.A., Lee, P.P., Flavell, E.R., Green, F.L., Flavell, J.H.: Young children’s understanding of intention. *Cognitive Development* 14(3), 463–486 (1999)
10. Fern, A., Natarajan, S., Judah, K., Tadepalli, P.: A decision-theoretic model of assistance. In: Proc. Int. Joint Conf. on Artificial Intelligence. pp. 1879–1884 (2007)
11. Garcia, J., Fernández, F.: Safe exploration of state and action spaces in reinforcement learning. *Journal of Artificial Intelligence Research* 45, 515–564 (2012)
12. Hayward, J.C.: Near miss determination through use of a scale of danger. Tech. rep., Pennsylvania State University PA, USA (1972)
13. Kaelbling, L.P., Littman, M.L., Cassandra, A.R.: Planning and acting in partially observable stochastic domains. *Artificial intelligence* 101(1-2), 99–134 (1998)
14. Kahneman, D.: Maps of bounded rationality: Psychology for behavioral economics. *The American economic review* pp. 1449–1475 (2003)
15. Kolter, J.Z., Ng, A.Y.: Near-bayesian exploration in polynomial time. In: Proc. Int. Conf. on Machine Learning. pp. 513–520. ACM (2009)
16. Lam, C.P., Yang, A.Y., Driggs-Campbell, K., Bajcsy, R., Sastry, S.S.: Improving human-in-the-loop decision making in multi-mode driver assistance systems using hidden mode stochastic hybrid systems. In: Proc. IEEE Int. Conf. on Intelligent Robots and Systems. pp. 5776–5783. IEEE (2015)
17. Nikolaidis, S., Kuznetsov, A., Hsu, D., Srinivasa, S.: Formalizing human-robot mutual adaptation: A bounded memory model. In: Proc. ACM/IEEE Int. Conf. on Human-Robot Interaction. pp. 75–82. IEEE Press (2016)
18. Nikolaidis, S., Ramakrishnan, R., Gu, K., Shah, J.: Efficient model learning from joint-action demonstrations for human-robot collaborative tasks. In: Proc. ACM/IEEE Int. Conf. on Human-Robot Interaction. pp. 189–196. ACM (2015)
19. Pedregosa, F., Varoquaux, G., Gramfort, A., Michel, V., Thirion, B., Grisel, O., Blondel, M., Prettenhofer, P., Weiss, R., Dubourg, V., Vanderplas, J., Passos, A., Cournapeau, D., Brucher, M., Perrot, M., Duchesnay, E.: Scikit-learn: Machine learning in Python. *Journal of Machine Learning Research* 12, 2825–2830 (2011)
20. Rasmussen, C.E.: Gaussian processes in machine learning. In: *Advanced lectures on machine learning*, pp. 63–71. Springer (2004)
21. Rubinstein, A.: *Modeling bounded rationality*. MIT press (1998)
22. Sadigh, D., Sastry, S.S., Seshia, S.A., Dragan, A.: Information gathering actions over human internal state. In: Proc. IEEE Int. Conf. on Intelligent Robots and Systems. pp. 66–73. IEEE (2016)
23. Sadigh, D., Sastry, S., Seshia, S.A., Dragan, A.D.: Planning for autonomous cars that leverage effects on human actions. In: Proc. Robotics: Science & Systems (2016)
24. Sunberg, Z.N., Ho, C.J., Kochenderfer, M.J.: The value of inferring the internal state of traffic participants for autonomous freeway driving. In: American Control Conference (ACC). pp. 3004–3010. IEEE (2017)
25. Vert, J.P., Tsuda, K., Schölkopf, B.: A primer on kernel methods. *Kernel methods in computational biology* 47, 35–70 (2004)



## 7 Appendix

### 7.1 Proof of Theorem 1

Theorem 1 is essentially a PAC bound, and the key to prove it is to show that at each time step our algorithm is  $\epsilon$ -optimistic with respect to the Bayes-optimal policy, and the value of optimism decays to zero given enough samples of unknown state action pairs.

It is obvious that the value of optimism of our algorithm (Equation 7) decays faster than the original POMDP-lite algorithm (Equation 4), since  $0 < p^G(x, a^R) < 1$ , which means strictly less reward bonus. In addition, the following lemma states that with proper choice of  $\beta$ , our algorithm generates a value function that is  $\epsilon$ -optimistic with respect to the Bayes-optimal policy.

**Lemma 1.** ( *$\epsilon$ -optimistic*) Let  $\tilde{V}^{G^*}(b_t, x_t)$  be the value function for our algorithm (with reward bonus), and let  $V^*(b_t, x_t)$  be the Bayes-optimal value function. If  $\beta = \frac{|X|^2|A^R|}{\phi(1-\gamma)^2}$ , then  $\forall x_t, \tilde{V}^{G^*}(b_t, x_t) \geq V^*(b_t, x_t) - \epsilon$ .

**Proof.** (Lemma 1) According to Equation 7, we have

$$\begin{aligned}
 \tilde{V}^{G^*}(b_t, x_t) &= \max_{a_t^R} \left\{ \frac{|X|^2|A^R|}{\phi(1-\gamma)^2} p^G(x_t, a_t^R) r^B(b_t, x_t, a_t^R) + r^R(b_t, x_t, a_t^R) + \right. \\
 &\quad \left. \sum_{x_{t+1}} \gamma P(x_{t+1}|b_t, x_t, a_t^R) \tilde{V}^{G^*}(b_t, x_{t+1}) \right\} \\
 &\geq \max_{a_t^R} \left\{ \frac{|X|^2|A^R|}{(1-\gamma)^2} r^B(b_t, x_t, a_t^R) + r^R(b_t, x_t, a_t^R) + \right. \\
 &\quad \left. \sum_{x_{t+1}} \gamma P(x_{t+1}|b_t, x_t, a_t^R) \tilde{V}^{G^*}(b_t, x_{t+1}) \right\} \\
 &\geq V^*(b_t, x_t) - \epsilon
 \end{aligned} \tag{7}$$

The second line follows from the fact that  $p^G(x_t, a_t^R) \geq \phi$ . The third line follows from Lemma 3 in [6].  $\square$

With Lemma 1, the analysis in the POMDP-lite paper [6] can be applied here, and thus proves our theorem.